Acta Crystallographica Section A
Foundations of Crystallography
ISSN 0108-7673

Received 16 November 2005
Accepted 11 May 2006

Calculation of spherical harmonics and Wigner *d* functions by FFT. Applications to fast rotational matching in molecular replacement and implementation into *AMoRe*

Stefano Trapani* and Jorge Navaza

Laboratoire de Virologie Moléculaire et Structurale, UMR 2472, CNRS, 1 Avenue de la Terrasse, Bâtiment 14B, 91198 Gif-sur-Yvette, France. Correspondence e-mail: trapani@vms.cnrs-gif.fr

The FFT calculation of spherical harmonics, Wigner D matrices and rotation function has been extended to all angular variables in the *AMoRe* molecular replacement software. The resulting code avoids singularity issues arising from recursive formulas, performs faster and produces results with at least the same accuracy as the original code. The new code aims at permitting accurate and more rapid computations at high angular resolution of the rotation function of large particles. Test calculations on the icosahedral IBDV VP2 subviral particle showed that the new code performs on the average 1.5 times faster than the original code.

1. Introduction

The rotation function, as defined by Rossmann & Blow (1962), measures the overlap between one Patterson function (the target object) and a rotated version of another (the search object) as a function of the rotation angle. The calculation of the overlap function can take advantage of spherical harmonic (SH) representation of the source and target objects if these are limited to a spherical domain. Using such representation, the overlap function $\mathcal{R}(\mathbf{R})$ ($\mathbf{R}$ being a rotation) can be expressed (Crowther, 1972) as

$$\mathcal{R}(\mathbf{R}) = \sum_{l=0}^{l_{\max}} \sum_{m_1,m_2=-l}^{l} C^l_{m_1,m_2} D^l_{m_1,m_2}(\mathbf{R}), \qquad (1)$$

which is an expansion in terms of the orthonormal Wigner D functions (the irreducible matrix representations of the rotation group). The sum truncation limit $l_{\max}$ is related to the angular resolution and is determined by the size and resolution of the superimposed functions according to the following formula:

$$l_{\max} \simeq 2\pi b/d_{\min} \quad (b\text{: radius;} \quad d_{\min}\text{: resolution}). \qquad (2)$$

Crowther (1972) showed the computational advantage of the SH approach in rotational search. If the Euler parametrization $\mathbf{R} \equiv \mathbf{R}(\alpha, \beta, \gamma)$ is used, separation of the three angular variables occurs, and a simple harmonic dependence for two of them results:

$$\mathcal{R}(\alpha, \beta, \gamma) = \sum_{l=0}^{l_{\max}} \sum_{m_1,m_2=-l}^{l} C^l_{m_1,m_2} d^l_{m_1,m_2}(\beta) \exp[i(m_1\alpha + m_2\gamma)]. \qquad (3)$$

This permits the fast calculation of β sections of the rotation function by two-dimensional fast Fourier transform (FFT). Evaluation of the reduced Wigner d functions for each β section is required.

Equation (1) requires the pre-calculation of the coefficients $C^l_{m_1,m_2}$. For Patterson overlap calculations, the $C^l_{m_1,m_2}$ coefficients can be efficiently computed using the formulas introduced by Navaza (1993):

$$C^l_{m_1,m_2} = \sum_{n=1}^{n_{\max}(l)} \overline{e^{(\text{target})}_{l,m_1,n}}\, e^{(\text{source})}_{l,m_2,n}, \qquad (4)$$

where the coefficients $e_{l,m,n}$ are given by

$$e_{l,m,n} = \frac{\{12\pi[2(l+2n)-1]\}^{1/2}}{V} \times \sum_{\mathbf{h}} \left[|F(\mathbf{h})|^2 Y_{l,m}(\hat{\mathbf{h}}) \frac{j_{l+2n-1}(2\pi hb)}{2\pi hb} \right] \qquad (5)$$

(F: structure factor; $\hat{\mathbf{h}}$: angular part of the reciprocal vector $\mathbf{h}$; $Y_{l,m}$: spherical harmonic of degree l and order m; j_l: spherical Bessel function of order l; b: integration radius; V: unit-cell volume). These formulas require that SH's be sampled on a non-regular angular grid corresponding to the reciprocal-lattice directions. Alternatively, to speed up calculations, a regular grid of SH values can be used to extract approximate values, provided that the grid sampling interval be sufficiently small.

The evaluation of SH's and Wigner functions – the former can be eventually reduced to special restrictions of the Wigner functions (see §2) – needed for the calculation of the rotation function are normally carried out using various recursive relationships (Edmonds, 1957; Courant & Hilbert, 1953; Altmann & Bradley, 1963; Risbo, 1996; Navaza, 1990). Recursion formulas, however, have singularities when β is a multiple of π, and care should be taken to ensure computa-

tional stability, especially at high angular resolutions. As an alternative to recursive formulas, Fourier synthesis is also employed by several authors from other fields for the calculation of SH's (see, for example, Dilts, 1985; Swarztrauber, 1984; Risbo, 1996), though, to our knowledge, only recently (Kovacs & Wriggers, 2002) has it been proposed for the calculation of the rotation function in crystallography. Fourier synthesis has the advantage of avoiding singularities and very finely sampled values can be rapidly obtained if FFT algorithms are used.

In this paper, we present the implementation of the Fourier representation of both the SH's and the reduced Wigner functions into the rotational search algorithms described above. The purpose of the work is to speed up the search procedures and to allow accurate computations of the rotation function at high angular resolutions. This will provide efficient algorithms for rotational searches with large particles like viruses. Two modifications in the search procedure are presented:

1. An accurate calculation of the coefficients $C^l_{m_1,m_2}$ is achieved at high angular resolutions by using FFT algorithms for SH sampling, avoiding the singularity issues of recursion formulas.

2. The Wigner d functions are substituted by their Fourier representation, which introduces a simple harmonic dependence on the β angular variable in the rotation function, thus allowing the FFT acceleration of all three rotational variables. This approach is equivalent to the fast rotational matching algorithm proposed by Kovacs & Wriggers (2002), who showed that the overlap function of two rotated bodies can be expressed as a three-dimensional Fourier sum if a rotation is factorized into the product of two rotations with a fixed angle $\beta = \pi/2$. We present here a more rapid implementation to obtain the Wigner function Fourier coefficients.

Implementation into the *AMoRe* molecular replacement package (Navaza, 1994) will be described.

2. Background

In this paper, the notation and the normalization conventions for SH's and Wigner functions are essentially those found in Navaza (2001), who refers to formulas reported in the book of Brink & Satchler (1968). A general introduction to Fourier analysis and representation theory can be found in Kirillov (1991).

The fundamental symmetry of a crystal is the periodicity, *i.e.* the invariance with respect to a particular group of translations. This symmetry is quite naturally displayed in terms of Cartesian coordinates and the basis functions for translations, *i.e.* the exponentials $\exp(2\pi i\mathbf{hx})$. The vector $\mathbf{h}$ of the reciprocal Bravais lattice labels the irreducible representations of the translation group, which are one-dimensional. The exponentials constitute a complete set of functions suited to expand any function that has the same periodicity as the crystal. In particular, the structure factors are the coefficients of the expansion of the electron density.

Analogously, spherical coordinates and the concomitant SH's are a very natural choice to represent any function bounded in space and displaying point-group rotational symmetry. Complex SH's $Y_{l,m}$ – where the integers l and m are the SH degree and order, respectively ($0 \le l < \infty$; $-l \le m \le l$) – are a complete basis for the irreducible representations of the infinite group of three-dimensional rotations, where, for each degree l, the corresponding SH's generate a $(2l+1)$-dimensional space which is rotationally invariant. When a system of spherical polar coordinates (θ, φ) is used, separation of variables occurs:

$$Y_{l,m}(\theta,\varphi) = i^l\left[\frac{2l+1}{4\pi}\frac{(l-m)!}{(l+m)!}\right]^{1/2} P_{l,m}(\cos\theta)\exp(im\varphi)$$

and a simple harmonic dependence on the longitude φ appears, while the dependence on the colatitude θ is related to the trigonometric associated Legendre functions (Brink & Satchler, 1968).

The Wigner D functions, which for a given degree l can be arranged as a square matrix $D^l_{m_1,m_2}$ of order $(2l+1)$ with indexes m_1 and m_2 running from $-l$ to $+l$, constitute the (irreducible) matrix representations of the rotation operators in the SH basis. If Euler angles (α, β, γ) are used to parametrize rotations, separation of variables occurs and a simple harmonic dependence on α and γ results:

$$D^l_{m_1,m_2}(\alpha,\beta,\gamma) = d^l_{m_1,m_2}(\beta)\exp[i(m_1\alpha + m_2\gamma)],$$

while the dependence of the reduced Wigner d functions on the nodal angle β is related to the Jacobi polynomials (Courant & Hilbert, 1953).

A simple relation exists between the $P_{l,m}(\cos\theta)$ and the d functions, as the former are proportional to the functions in the central column of the d^l matrices:

$$P_{l,m}(\cos\theta) = \left[\frac{(l+m)!}{(l-m)!}\right]^{1/2} d^l_{m,0}(\theta).$$

Therefore, the computation of both SH's and Wigner functions can be reduced to the computation of the reduced d functions.

The explicit expression given by Wigner for the d functions (Brink & Satchler, 1968) is computationally cumbersome and cannot be effectively implemented as is. Instead, recursive formulas derived from it – along the degree l and/or the order m_1, m_2 directions of the d-matrix 'pyramid' – are normally used. The literature on the subject is sparse (Edmonds, 1957; Courant & Hilbert, 1953; Altmann & Bradley, 1963; Risbo, 1996; Navaza, 1990)

Since the $d(\beta)$ matrices become diagonal when $\beta = 0$ or π, recursive formulas present singularities at these points, and care must be taken to ensure computational stability around them. Risbo (1996) proposed a binomial recursion, which he reported to be stable up to at least $l = 360$. The binomial recursion can be reconducted to a nine-term $l \rightarrow l+1$ recursion where each element of degree $l+1$ in the d pyramid receives contributions from the nine adjacent elements at level l. Navaza (1990) proposed a three-term monodimensional

recursion in the m_1 direction [see also equations (15)–(16) in Appendix *A* of the present article]. If computation is carried out on a logarithmic scale, storing separately the mantissas and exponents as double-precision and integer numbers, respectively, this recursion has proven to be quite stable at least up to $l = 1000$ for angles greater than 10^{-5} rad. This recursion can be found implemented in the *AMoRe* package.

3. Methods

3.1. FFT calculation of the *d* functions

The expression for the Fourier representation of the d functions is given by Edmonds (1957), who based it on unpublished notes by E. Wigner. It can also be found in Risbo (1996). By factorization of a nodal rotation,

$$\mathbf{R}(0, \beta, 0) = \mathbf{R}(-\tfrac{\pi}{2}, 0, 0)\mathbf{R}(0, -\tfrac{\pi}{2}, 0) \times \mathbf{R}(\beta, 0, 0)\mathbf{R}(0, \tfrac{\pi}{2}, 0)\mathbf{R}(\tfrac{\pi}{2}, 0, 0),$$

and using the corresponding similarity transformation of the representative D^l matrices, one obtains the Fourier decomposition of the d functions:

$$d^l_{m_1,m_2}(\beta) = i^{m_2-m_1} \sum_{u=-l}^{+l} d^l_{u,m_1}(\tfrac{\pi}{2}) d^l_{u,m_2}(\tfrac{\pi}{2}) \exp(iu\beta) = \sum_{u=-l}^{+l} B^l_{m_1,m_2,u} \exp(iu\beta) \quad (6)$$

with the Fourier coefficients given by

$$B^l_{m_1,m_2,u} = i^{m_2-m_1} d^l_{u,m_1}(\tfrac{\pi}{2}) d^l_{u,m_2}(\tfrac{\pi}{2})$$

or, defining the matrix $\Delta^l \equiv d^l(\frac{\pi}{2})$,

$$B^l_{m_1,m_2,u} = i^{m_2-m_1} \Delta^l_{u,m_1} \Delta^l_{u,m_2}, \quad (7)$$

where the index u labels the frequency in β.

Equation (6) shows that the d functions of degree l are (at least) 2π periodic and band limited, with $(2l + 1)$ Fourier components. The following properties hold.

1. Since the d's are real-valued functions, the hermitian relationship $B^l_{m_1,m_2,-u} = \overline{B^l_{m_1,m_2,u}}$ holds, and only the $(l + 1)$ non-negative or non-positive frequencies are non-redundant. This is analogous to Friedel's law which stipulates that the structure factor obtained by changing the signs of the Miller indices is equal to the complex conjugate of the original one.

2. Since the d functions are either even or odd, depending on the parity of $(m_1 - m_2)$, their Fourier components are either real or pure imaginary numbers, respectively. Thus, from equation (7), the Fourier coefficients can be computationally stored as real numbers $b^l_{m_1,m_2,u}$ given by

$$b^l_{m_1,m_2,u} = (-1)^{\mathrm{int}[(m_2-m_1)/2]} \Delta^l_{u,m_1} \Delta^l_{u,m_2}. \quad (8)$$

Furthermore, d values need to be sampled over the half-period interval $[0, \pi)$ only.

3. Systematic absences are found in the frequencies of the central column/row of the d matrices (*i.e.* of the SH associated Legendre functions): from equations (22) and (23), it follows that, for d^l_{0,m_2} and $d^l_{m_1,0}$, all odd frequencies disappear when l is odd, and the same happens to even frequencies when l is even. In the latter case, the corresponding d functions are π periodic.

The d functions of degree l can therefore be sampled on $N \geq l$ points in the interval $[0, \pi)$ {or $N/2 \geq l/2$ points in the interval $[0, \pi/2)$ when $m_2 = 0$ and l is even} using FFT algorithms optimized for even/odd real functions. In the present work, we have written a Fortran code linked to the *FFTW* (version 3.0.1) library of routines (Frigo & Johnson,

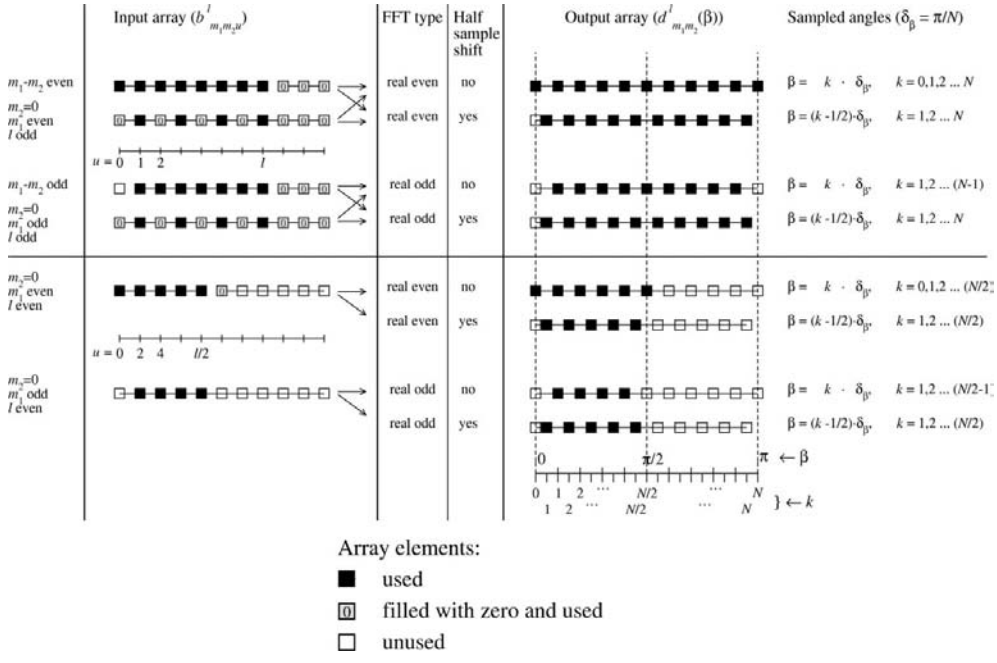

Figure 1
Scheme of the array arrangement used for the FFT *d*-function calculation.

1998) for the calculation of the d functions. Fig. 1 shows a scheme of the different types of routines and array arrangements that can be used.

3.2. Calculation of the Fourier coefficients of the *d* functions

According to equations (7) and (8), the Fourier coefficients of the $d(\beta)$ functions can be obtained in a straightforward way by calculating these functions for the particular argument $\beta = \pi/2$. The successive multiplication of the two columns m_1 and m_2 of the resulting Δ^l matrix gives a real-number representation of the $d^l_{m_1,m_2}$ Fourier spectrum. The Δ matrices represent a computationally convenient way of storing the Fourier coefficients, for a given degree l, as a two-dimensional array ($\Delta^l_{u,m}$), instead of a three-dimensional array ($b^l_{m_1,m_2,u}$). Since only $(l+1)$ frequencies are relevant, only the bottom halves ($u \geq 0$) of the Δ matrices need to be calculated. Furthermore, explicit calculation of the $\Delta^l_{u,m}$ coefficients can be limited to the 'asymmetric triangle' $0 \leq u \leq m_2 \leq l$ (which represents $\sim 1/8$ of the whole matrix) and then extended by symmetry (see Appendix A) to the rest of the matrix.

Calculation of the Δ matrices can be performed by adapting the available d-matrix recursive formulas for $\beta = \pi/2$. In this work, we use two two-term recursions in the l direction for the bottom rows of the matrices and one three-term recursion in the column direction:

$$\Delta^l_{l,0} = -\left(\frac{2l-1}{2l}\right)^{1/2} \Delta^{l-1}_{l-1,0}, \tag{9}$$

$$\Delta^l_{l,m_2} = \left[\frac{(l/2)(2l-1)}{(l+m_2)(l+m_2-1)}\right]^{1/2} \Delta^{l-1}_{l-1,m_2-1}, \tag{10}$$

$$\Delta^l_{m_1,m_2} = \frac{2m_2}{[(l-m_1)(l+m_1+1)]^{1/2}} \Delta^l_{m_1+1,m_2} - \left[\frac{(l-m_1-1)(l+m_1+2)}{(l-m_1)(l+m_1+1)}\right]^{1/2} \Delta^l_{m_1+2,m_2} \tag{11}$$

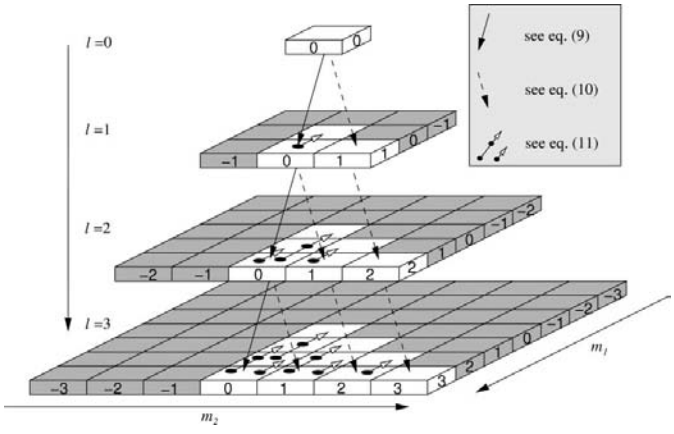

Figure 2
Schematic representation of the recursions used for the calculation of the Δ-matrix pyramid. White blocks are calculated explicitly, while dark blocks can be obtained by symmetry.

with initial condition

$$\Delta^0_{0,0} = 1. \tag{12}$$

Equations (9), (10) and (12) are easily obtained from the initialization equation (16), while equation (11) is obtained from the recursion formula (15). Recursion (11) is the most prone to error accumulation. In order to improve computational accuracy, it can be carried out using logarithmic arithmetic, storing in separate variables the mantissas and exponents of numbers (Navaza, 1990). Using the above formulas, the asymmetric triangles of the Δ matrices can be calculated recursively using the scheme depicted in Fig. 2.

If matrices of even degree only are needed (which is the case for the Patterson-correlation rotation function), equations (9) and (10) can be replaced by three $l \rightarrow l+2$ recursions:

$$\Delta^l_{l,0} = \left[\frac{(2l-1)(2l-3)}{4l(l-1)}\right]^{1/2} \Delta^{l-2}_{l-2,0},$$

$$\Delta^l_{l,1} = \left[\frac{(2l-1)(2l-3)}{4(l-2)(l+1)}\right]^{1/2} \Delta^{l-2}_{l-2,1},$$

$$\Delta^l_{l,m_2} = \left[\frac{(l/2)(2l-1)(l-1)(2l-3)}{2(l+m_2)(l+m_2-1)(l+m_2-2)(l+m_2-3)}\right]^{1/2} \times \Delta^{l-2}_{l-2,m_2-2},$$

while maintaining equation (11) and with initial conditions ($l = 2$):

$$\Delta^2_{2,0} = \tfrac{6^{1/2}}{4}; \quad \Delta^2_{2,1} = -\tfrac{1}{2}; \quad \Delta^2_{2,2} = \tfrac{1}{4}.$$

3.3. Three-dimensional FFT calculation of the rotation function (fast rotational matching)

When equation (3) is modified by the introduction of the Fourier representation of the Wigner d functions, one obtains a three-dimensional Fourier expression for the rotation function:

$$\mathcal{R}(\alpha,\beta,\gamma) = \sum_{m_1=-l_{\max}}^{l_{\max}} \sum_{u=-l_{\max}}^{l_{\max}} \sum_{m_2=-l_{\max}}^{l_{\max}} W_{m_1,u,m_2} \exp[i(m_1\alpha + u\beta + m_2\gamma)], \tag{13}$$

where the rotation-function Fourier coefficients $W^l_{m_1,u,m_2}$ are given by

$$W_{m_1,u,m_2} = \sum_{l=l_{\min}}^{l_{\max}} C^l_{m_1,m_2} B^l_{m_1,m_2,u} = i^{m_2-m_1} \sum_{l=l_{\min}}^{l_{\max}} C^l_{m_1,m_2} \Delta^l_{u,m_1} \Delta^l_{u,m_2} \tag{14}$$

with $l_{\min} = \max(|m_1|, |m_2|, |u|)$. Therefore, three-dimensional FFT algorithms can be used for the rapid evaluation of the rotation function.

It is convenient to think of $\mathcal{R}(\alpha, \beta, \gamma)$ as a real periodic function defined in the Euler coordinate space. The following properties hold.

- Hermiticity of the Fourier coefficients:

$$W_{-m_1,-u,-m_2} = \overline{W}_{m_1,u,m_2}.$$

- According to equation (13), the period of the rotation function is 2π along the three directions (α, β, γ). However, if the target and search Patterson functions have rotational symmetry along z of order n_t and n_s respectively, the periodicity is $2\pi/n_s$ and $2\pi/n_t$ along α and γ, respectively. Correspondingly, systematic absences are present in the rotation-function Fourier spectrum if $m_1 \not\equiv 0 \bmod n_t$ or $m_2 \not\equiv 0 \bmod n_s$.

- Since the rotations (α, β, γ) and $(\alpha + \pi, -\beta, \gamma + \pi)$ are equivalent, only half a period in the β direction is non-redundant. This equivalence can be considered as a diagonal glide-plane symmetry placed at $\beta = 0$ in Euler space. It results, in Fourier space, in the following parity relationship in the u direction:

$$W_{m_1,-u,m_2} = (-1)^{m_1-m_2} W_{m_1,u,m_2}$$

and in some systematic absences in the (m_1, m_2) plane:

$$W_{m_1,0,m_2} = 0 \quad \text{if} \quad (m_1 - m_2) \quad \text{odd}.$$

Using the above properties, the following procedure can be implemented to conveniently calculate the rotation function by three-dimensional FFT:

1. Calculate the 'semi-pyramidal' array of the real Δ matrices:

$$\Delta^l_{u,m}, \quad \begin{cases} 2 \le l \le l_{\max}, & l \text{ even} \\ 0 \le u \le l \\ -l \le m \le l \end{cases}$$

as described in §3.2.

2. Calculate the 'semi-pyramidal' array of the complex coefficients:

$$C^l_{m_1,m_2} = (C^R)^l_{m_1,m_2} + i(C^I)^l_{m_1,m_2},$$
$$\begin{cases} 2 \le l \le l_{\max}, & l \text{ even} \\ 0 \le m_1 \le l, & m_1 \equiv 0 \bmod n_t \\ -l \le m_2 \le l, & m_2 \equiv 0 \bmod n_s \end{cases}$$

(where the superscripts R and I indicate the real and imaginary components, respectively) using equations (4) and (5). FFT sampling of SHs can be used to evaluate equation (5), as described in §3.1.

3. Calculate two non-redundant octants of Fourier coefficients:

$$W_{m_1,u,m_2} = W^R_{m_1,u,m_2} + i\, W^I_{m_1,u,m_2}, \quad \begin{cases} 0 \le m_1 \le l_{\max} \\ 0 \le u \le l_{\max} \\ -l_{\max} \le m_2 \le l_{\max}. \end{cases}$$

The real and imaginary components of the Fourier coefficients can be calculated using equation (14) and according to the following scheme (indices have been omitted for convenience):

$(m_2 - m_1) \bmod 4$	W^R	W^I
0	$\sum C^R \Delta\Delta$	$\sum C^I \Delta\Delta$
1	$-\sum C^I \Delta\Delta$	$\sum C^R \Delta\Delta$
2	$-\sum C^R \Delta\Delta$	$-\sum C^I \Delta\Delta$
3	$\sum C^I \Delta\Delta$	$-\sum C^R \Delta\Delta.$

4. Make a three-dimensional hermitian FFT:

$$W_{m_1,u,m_2} \xrightarrow{\text{hermitian 3D FFT}} \mathcal{R}(\alpha, \beta, \gamma).$$

By exploiting the diagonal glide symmetry of the rotation function, one can restrict the calculation to the non-redundant interval $0 \le \beta \le \pi$. Also, if memory limitations require it, steps 3 and 4 can be carried out in bunches, storing and retrieving the results from disk.

4. Results

In the present work, we have implemented the Fourier representation of SH and Wigner functions in the rotational search procedure of the molecular replacement software *AMoRe*.

1. A general-purpose Fortran code has been written for the calculation of the Δ matrices and for the FFT sampling of SH and Wigner functions; the code computes the Δ matrices using double-precision or logarithmic double-precision arithmetic. FFT calculations can be performed using single- or double-precision arithmetic.

2. SH FFT sampling has been introduced in *AMoRe* for the calculation of the coefficients $C^l_{m_1,m_2}$.

3. FFT acceleration of the β angular variable for the calculation of the rotation function, as described in §3.3, has been introduced in *AMoRe*.

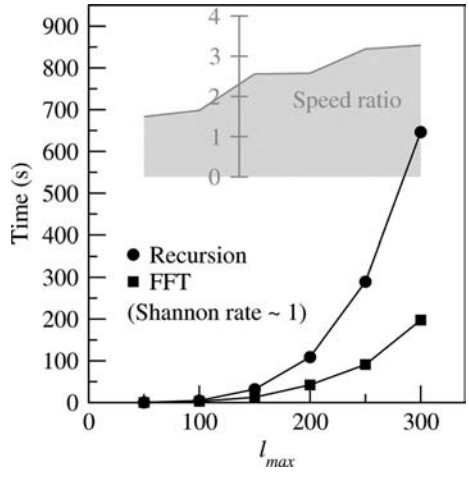

Figure 3
Time performance of d-matrix calculations. Time refers to the cumulate computation time for all even-degree d matrices (one asymmetric triangle) up to $l = l_{\max}$. Recursive and Δ-matrix calculations were performed in double-precision logarithmic mode. FFT calculations were performed in double-precision mode.

The developed code has been linked to routines from the *FFTW* library, version 3.0.1 (Frigo & Johnson, 1998). In order to test the *AMoRe* code performance, self-rotation function calculations have been carried out using the crystallographic data of the icosahedral IBDV VP2 subviral particle (Coulibaly *et al.*, 2005) (PDB ID: 1WCD). Calculations were performed on a Linux AMD Athlon(tm) MP 2400+ PC with 2 Gb RAM.

4.1. Time performance of the SH and *d*-function FFT calculation

Fig. 3 shows a comparison between the recursive and FFT computation times for d matrices. Calculations were performed using the highest precision and the minimum Shannon rate allowed by the code. We will denote as 'speed ratio' the computing time spent when using the recursive formulas divided by the time spent when using the FFT approach:

$$\text{speed ratio} = \frac{\text{recursion-based calculation time}}{\text{FFT-based calculation time}}.$$

A speed ratio between 1.5 and 3.2 was observed for the cumulate calculation of all even-degree d functions with $l_{\max}$ ranging from 50 to 300. Better results were obtained at Shannon rates higher than 1 (Fig. 4).

When the calculation was limited to the central column of the d matrices, in order to obtain the SH's, the speed of the FFT calculation was comparable with or better than that of the recursive calculation for Shannon rates higher than 2. In the case of the rotation-function $C^l_{m_1,m_2}$ coefficients, which require a very fine SH sampling, a speed ratio between 1.5 and 2.4 was observed for the SH calculation at a Shannon rate of ~ 10 and for $l_{\max}$ up to 1000.

The FFT-based computations include an initialization step where the Δ matrices and the FFT plans are evaluated. Four types of FFT plans, whose sizes depend on the Shannon rate and $l_{\max}$, need to be evaluated for even-l calculations (Fig. 1), and one Δ matrix for each degree l (up to $l_{\max}$) needs to be calculated. The time required for the initialization step contributes differently to the overall computation time when one compares the SH (*i.e.* one d-matrix column) and the whole d-matrix calculation. This accounts for the lower speed-up observed for the SH FFT calculation. While for d matrices the initialization step represented, in the tested cases, less than 5% of the total computation time, during SH calculations the initialization step required 50 to 67% of the total time.

4.2. Accuracy of the SH FFT calculation

Accuracy of the SH FFT calculation has been estimated by calculating the deviation from unity of the norm of the d-matrix central columns. The norm deviations for the first sampled angles (the angles closest to zero) at a high Shannon rate (~ 10) were smaller than 10^{-10} for l up to 1000 (Fig. 5). These norm deviations are slightly better than those observed for d values calculated by recursion formulas.

4.3. Calculation of the rotation-function $C^l_{m_1,m_2}$ coefficients using SH FFT values

No significant speed improvement during the *AMoRe* $C^l_{m_1,m_2}$ calculation was observed after the SH recursive algorithm was substituted for the SH FFT calculation. Accuracy of the calculation seemed to be maintained, as could be seen from a comparison of the rotational search results (see below).

4.4. Three-dimensional FFT rotation-function calculation

The self-rotation function of the icosahedral IBDV VP2 subviral particle was calculated at different resolution limits and with different integration radii (Table 1), corresponding to a SH expansion limit $l_{\max}$ varying from 52 to 178.

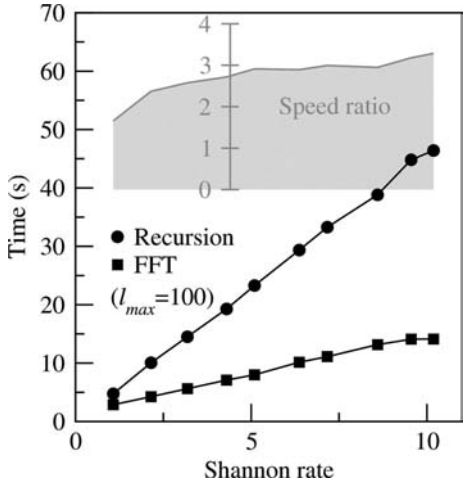

Figure 4
Time performance of d-matrix calculations as a function of the Shannon rate. Time refers to the cumulate computation time of all even-degree d matrices (one asymmetric triangle) up to $l_{\max} = 100$. Recursive and Δ-matrix calculations were performed in double-precision logarithmic mode. FFT calculations were performed in double-precision mode.

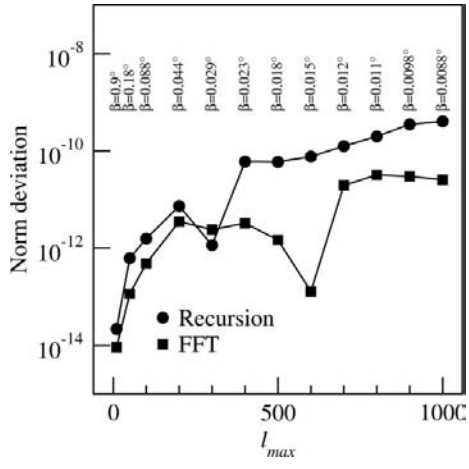

Figure 5
Accuracy of SH calculations. The deviation from unity of the modulus of the central column of the d matrices is reported as a function of $l_{\max}$. The values are calculated with respect to the first sampled angle (the angle closest to zero) at a Shannon rate of ~ 10. Recursive and Δ-matrix calculations were performed in double-precision logarithmic mode. FFT calculations were performed in double-precision mode.

Table 1
Time performance for the calculation of the self-rotation function of the IBDV VP2 subviral particle.

PDB ID	1WCD
Space group	$P6_3$
Unit cell	$a = b = 258.9, c = 347.3$ Å

				Self-rotation function calculation (using pre-calculated $C^l_{m_1,m_2}$'s)			Complete rotational search (including $C^l_{m_1,m_2}$ computation and peak search)		
				Time (s)			Time (s)		
l_{max}	N_β†	b (Å)	d_{min} (Å)	using 2D FFT‡	using 3D FFT‡	Speed ratio	using 2D FFT‡	using 3D FFT‡	Speed ratio
52	72	90	10.0	0.410	0.110	3.73	1.38	1.05	1.31
52	144	90	10.0	1.04	0.445	2.35	2.22	1.60	1.39
64	72	110	10.0	0.737	0.198	3.72	2.20	1.58	1.39
64	144	110	10.0	1.67	0.549	3.04	3.35	2.16	1.55
66	72	90	8.0	0.791	0.194	4.08	3.32	2.69	1.24
66	144	90	8.0	1.80	0.517	3.48	4.55	3.20	1.42
76	90	130	10.0	1.49	0.288	5.19	3.73	2.39	1.56
76	180	130	10.0	3.46	1.05	3.29	6.13	3.63	1.69
80	90	110	8.0	1.72	0.367	4.66	5.71	4.27	1.34
80	180	110	8.0	3.89	1.02	3.83	8.34	5.36	1.56
88	108	90	6.0	2.89	0.495	5.83	13.1	10.7	1.23
88	216	90	6.0	6.55	1.75	3.73	17.6	12.8	1.37
88	108	150	10.0	2.87	0.50	5.76	5.98	3.42	1.75
88	216	150	10.0	6.54	1.67	3.92	10.5	5.44	1.93
96	108	130	8.0	3.46	0.805	4.30	9.52	6.66	1.43
96	216	130	8.0	7.70	1.95	3.94	14.6	8.62	1.69
106	144	90	5.0	6.33	1.16	5.47	32.5	27.7	1.17
106	270	90	5.0	13.5	3.41	3.96	41.3	31.7	1.30
108	144	110	6.0	6.76	1.22	5.54	23.6	18.1	1.30
108	270	110	6.0	14.4	3.47	4.15	32.8	22.0	1.50
110	144	150	8.0	7.21	1.29	5.58	16.1	9.83	1.63
110	270	150	8.0	14.9	3.76	3.96	25.4	13.9	1.83
128	144	130	6.0	12.3	2.33	5.26	38.7	28.9	1.34
128	288	130	6.0	26.6	5.11	5.22	55.0	33.5	1.64
130	144	110	5.0	12.8	2.63	4.87	56.3	47.3	1.19
130	288	110	5.0	27.6	5.47	5.05	73.3	52.2	1.41
148	162	150	6.0	24.4	4.00	6.09	61.8	41.7	1.48
148	324	150	6.0	51.9	8.46	6.17	92.1	49.0	1.88
154	180	130	5.0	28.8	4.93	5.84	97.5	74.2	1.31
154	360	130	5.0	62.1	10.9	5.71	135.1	84.2	1.60
178	216	150	5.0	56.6	8.95	6.32	172.6	126.6	1.36
178	432	150	5.0	121.0	20.1	6.04	243.9	144.6	1.69

† Number of β sample points in $[0, \pi)$ ‡ Fourier coefficient calculations carried out at the maximum precision allowed by the code. FFT calculations carried out in single-precision mode.

In all tested cases, all the NCS axes of the icosahedral particle could be found. When the results obtained with the original *AMoRe* program were compared with those obtained with the new code, no difference was found in the angular parameters and height of the corresponding rotation-function peaks, even when single-precision FFT routines were used, showing that the new code produced results with the same accuracy.

Table 1 compares the time performance of the classical two-dimensional and the new three-dimensional rotational search procedure applied to the 1WCD data. A general improvement of the calculation speed was observed using β samplings corresponding to Shannon rates between 1 and 2. The time spent in a complete rotation-function calculation, including the computation of the $C^l_{m_1,m_2}$ coefficients and the peak-search procedure, resulted in a time divided by a factor of 1.48 on the average. When using precalculated $C^l_{m_1,m_2}$ coefficients, as *AMoRe* often does, the FFT procedure was up to six times faster, with an average speed ratio of 4.7.

As shown in Table 1, the computation of the $C^l_{m_1,m_2}$'s is the most time consuming part of rotation-function calculations. The use of the FFT technique to calculate the SH's gives greater stability and accuracy but no appreciable gain in time. With stored $C^l_{m_1,m_2}$'s, the rotation function depends on the molecular size and the resolution only through $l_{max} = 2\pi b/d_{min}$ [equation (2)] and the chosen Shannon rate (typically 1.5 in *AMoRe*). Thus, the results of columns 5 to 7 in Table 1 are model independent. For smaller structures, smaller l_{max}'s are often used, and this results in smaller speed ratios than those reported in Table 1. For example, calculations performed with $l_{max} = 40$ resulted in speed ratios of 2.21 and 1.40 using Shannon rates of 1 and 2, respectively.

5. Discussion

We have extended to all angular variables and implemented into *AMoRe* the Fourier representation of SH, D matrices and rotation function. The new code produces results with at least

the same accuracy as the original code, avoids singularity issues arising from recursion formulas, and has a better time performance. Improvement in speed is due essentially to the three-dimensional FFT rotation function calculation and, in the tested cases, calculation times were divided by factors ranging between 1.17 and 1.93.

We have made a comparison between Kovacs & Wriggers's (2002) and our three-dimensional FFT rotational search procedure, and we observed that the two codes perform with comparable speed, with a slightly better performance of our code owing to a more efficient planning of the FFT. The speed improvements they reported are higher than ours, though using a different set of test data. However, their results were obtained by comparison with a two-dimensional procedure that used the rather slow binomial recursion (Risbo, 1996) to calculate the d matrices, while our two-dimensional results are based on the much faster recursion formulas proposed by Navaza (1990).

APPENDIX A
The reduced Wigner d^l matrices

The reduced Wigner $d^l(\beta)$ matrices ($l = 0, 1, \ldots, \infty$) are squared real unitary matrices of order $(2l + 1)$, with row and column indices m_1, m_2 running conventionally from $-l$ to $+l$. The elements $d^l_{m_1,m_2}(\beta)$ are functions of the angular variable β and can be defined by the following three-term recurrence relation:

$$d^l_{m_1,m_2}(\beta) = \frac{2[m_2 - (m_1+1)\cos(\beta)]}{[(l-m_1)(l+m_1+1)]^{1/2}\sin(\beta)} d^l_{m_1+1,m_2}(\beta) - \left[\frac{(l-m_1-1)(l+m_1+2)}{(l-m_1)(l+m_1+1)}\right]^{1/2} d^l_{m_1+2,m_2}(\beta) \quad (15)$$

with initial values (bottom row):

$$d^l_{l,m_2}(\beta) = (-1)^{l-m_2}\left[\frac{(2l)!}{(l-m_2)!(l+m_2)!}\right]^{1/2} \times \left(\sin\frac{\beta}{2}\right)^{l-m_2}\left(\cos\frac{\beta}{2}\right)^{l+m_2}. \quad (16)$$

The d matrices have the following properties.

- Symmetry with respect to the diagonals/centre:

$$d^l_{-m_1,-m_2}(\beta) = d^l_{m_2,m_1}(\beta) = (-1)^{m_1-m_2} d^l_{m_1,m_2}(\beta). \quad (17)$$

- Symmetry with respect to the central column/row:

$$d^l_{m_1,m_2}(\beta \pm \pi) = (-1)^{l-m_2} d^l_{m_1,-m_2}(\beta) = (-1)^{l-m_1} d^l_{-m_1,m_2}(\beta) \quad (18)$$

and, for $\beta = \pi/2$,

$$d^l_{m_1,m_2}(\pi/2) = (-1)^{l-m_1} d^l_{m_1,-m_2}(\pi/2) = (-1)^{l-m_2} d^l_{-m_1,m_2}(\pi/2). \quad (19)$$

- Parity:

$$d^l_{m_1,m_2}(-\beta) = (-1)^{m_1-m_2} d^l_{m_1,m_2}(\beta). \quad (20)$$

- β-shift symmetry/periodicity:

$$d^l_{m_1,m_2}(\beta + 2\pi) = d^l_{m_1,m_2}(\beta) \quad (21)$$

and, for m_1 or $m_2 = 0$ (central row/column),

$$d^l_{0,m_2}(\beta + \pi) = (-1)^l d^l_{0,m_2}(\beta), \quad (22)$$

$$d^l_{m_1,0}(\beta + \pi) = (-1)^l d^l_{m_1,0}(\beta). \quad (23)$$

This work was funded by Human Frontier Science Program RGP0026/2003. We acknowledge Dr Willy R. Wriggers and Dr Julio Kovacs for providing their three-dimensional fast rotational matching code for comparison and for discussion. We acknowledge Dr Leandro F. Estrozi for useful discussion.

References

Altmann, S. L. & Bradley, C. J. (1963). *Philos. Trans. R. Soc. London Ser. A*, **255**, 193–198.
Brink, D. M. & Satchler, G. R. (1968). *Angular Momentum*, 2nd ed. Oxford University Press.
Coulibaly, F., Chevalier, C., Gutsche, I., Pous, J., Navaza, J., Delmas, B. & Rey, F. A. (2005). *Cell*, **120**, 761–772.
Courant, R. & Hilbert, D. (1953). *Methods of Mathematical Physics*, Vol. 1. New York: Interscience Publishers.
Crowther, R. A. (1972). *The Molecular Replacement Method*, edited by M. G. Rossmann. *International Science Reviews Series*, Vol. 13, pp. 173–178. New York: Gordon and Breach.
Dilts, G. A. (1985). *J. Comput. Phys.* **57**, 439–453.
Edmonds, A. R. (1957). *Angular Momentum in Quantum Mechanics.* New York: Princeton University Press.
Frigo, M. & Johnson, S. G. (1998). Proceedings of ICASSP, Vol. 3, pp. 1381–1384.
Kirillov, A. A. (1991). Editor. *Representation Theory and Noncommutative Harmonic Analysis I: Fundamental Concepts. Encyclopedia of Mathematical Science*, Vol. 22. Berlin: Springer-Verlag.
Kovacs, J. A. & Wriggers, W. (2002). *Acta Cryst.* D**58**, 1282–1286.
Navaza, J. (1990). *Acta Cryst.* A**46**, 619–620.
Navaza, J. (1993). *Acta Cryst.* D**49**, 588–591.
Navaza, J. (1994). *Acta Cryst.* A**50**, 157–163.
Navaza, J. (2001). *Crystallography of Biological Macromolecules*, *International Tables for Crystallography*, Vol. F, edited by M. G. Rossmann & E. Arnold, pp. 269–274. International Union of Crystallography.
Risbo, T. (1996). *J. Geodesy*, **70**, 383–396.
Rossmann, M. G. & Blow, D. M. (1962). *Acta Cryst.* **15**, 24–31.
Swarztrauber, P. N. (1984). *Large Scale Scientific Computation*, pp. 271–299. New York: Academic Press.